



OPEN

TR-FRET Assays of Huntingtin Protein Fragments Reveal Temperature and PolyQ Length-Dependent Conformational Changes

SUBJECT AREAS:
IMMUNOCHEMISTRY
NEURODEGENERATIVE
DISEASESReceived
28 November 2013Accepted
19 June 2014Published
7 July 2014Correspondence and
requests for materials
should be addressed to
Y.D. (yuding@fudan.
edu.cn) or B.L.
(luboxun@fudan.edu.
cn)* These authors
contributed equally to
this work.

Xiaotian Cui*, Qingnan Liang*, Yijian Liang*, Mingxing Lu*, Yu Ding & Boxun Lu

State Key Laboratory of Genetic Engineering, School of Life Sciences, Fudan University, Shanghai, China.

Time-Resolved Fluorescence Resonance Energy Transfer (TR-FRET) technology is a widely used immunoassay that enables high-throughput quantitative measurements of proteins of interest. One of the well established examples is the TR-FRET assay for mutant huntingtin protein (HTT), which is the major cause of the neurodegenerative Huntington's disease (HD). To measure the mutant HTT protein, the published assays utilize a polyQ antibody, MW1, paired with HTT N-terminal antibodies. MW1 has much higher apparent affinity to mutant HTT with expanded polyQ stretch than to wild-type HTT with shorter polyQ, and thus the assays detect mutant HTT preferentially. Here we report a reversible temperature dependent change of TR-FRET signals for HTT N-terminal fragments: the signals become higher when the temperature is lowered from room temperature to 4 °C. Interestingly, the temperature sensitivity of the TR-FRET signals is much higher for the Q25 (wild-type) than for the Q72 (mutant) protein. We further revealed that it is likely due to a temperature and polyQ length-dependent structural or spatial change of HTT, which is potentially useful for understanding polyQ structure and toxicity.

High-throughput quantitative measurements of protein levels enable scientists to screen for genetic modifiers or drugs that regulate the abundance of the proteins of interest, and thus are desired for both basic and translational research. One of the most widely used technology developed for such purposes is the Time Resolved-Fluorescence Resonance Energy Transfer (TR-FRET)^{1,2}. FRET is based on the transfer of energy between two fluorophores in close proximity (5 ~ 9 nm), referred to as a donor and an acceptor. Excitation of the donor by an energy source triggers an energy transfer towards the acceptor, which in turn emits specific fluorescence at a given wavelength. Traditional FRET signals are influenced by background fluorescence from sample components, which is extremely transient and thus can be eliminated using time-resolved methodologies (Fig. 1a). TR-FRET uses a rare earth complex as the donor, which gives long-lived fluorescence signals peak at 615 nm upon excitation by an energy pulse. As a result, TR-FRET acceptors emit long-lived fluorescence peak at 665 nm only when engaged in a FRET process. Thus, a time delay of approximately 50 to 150 μs between the system excitation and fluorescence measurement could be introduced to eliminate non-specific short-lived emissions (Fig. 1a). By using the acceptor conjugated and the donor conjugated antibodies targeting the same protein, the TR-FRET signals are generated only when the two antibodies bind with the same protein molecule. As a result, the TR-FRET signals are in proportion to the target protein concentration and could be used to quantify its level (Fig. 1). The technology has been successfully applied to the measurement of the mutant huntingtin protein (HTT)^{3,4}, which has a polyQ length longer than 36 and causes of the neurodegenerative Huntington's disease (HD)⁵.

To measure mutant HTT proteins, the published assays use a polyQ antibody, MW1⁶, as the acceptor conjugated antibody. MW1 has much higher apparent affinity to longer polyQ than shorter polyQ, and thus preferentially detects mutant HTT proteins⁷⁻⁹ (Fig. 1b). As a result, when utilizing MW1 as the acceptor antibody, it could be paired with other HTT antibodies (such as 2B7 and 4C9, Fig. 1b) to preferentially detect mutant HTT proteins over wild-type HTT proteins⁴.

HTT N-terminal fragments, such as the HTT-exon1 fragments, are present in HD patients due to HTT protein cleavage or splicing^{10,11}. These fragments have been widely used to model the disease in both animal and cellular

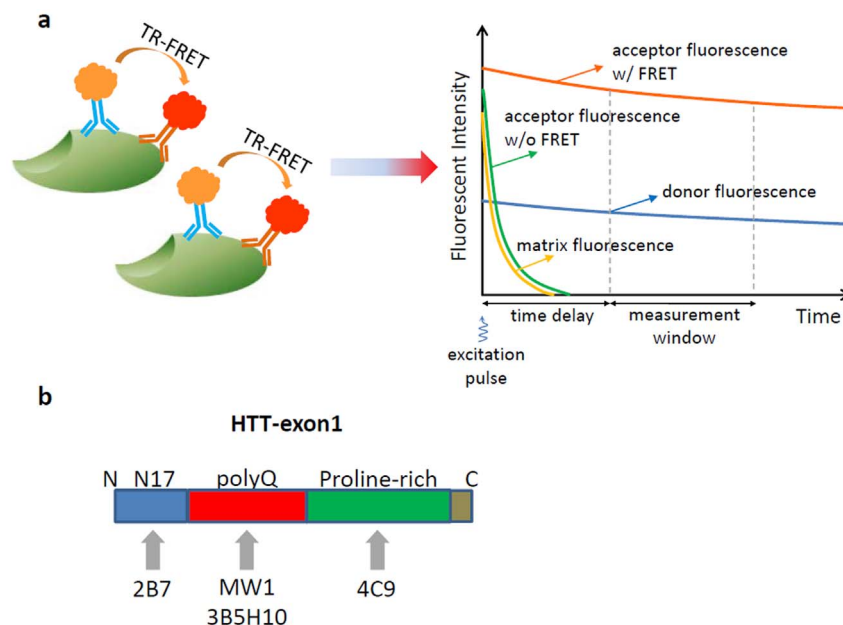


Figure 1 | Principles of TR-FRET measurement of the protein level. (a) *Left:* binding of two antibodies to the same protein molecule allow sufficient spatial proximity that enables fluorescence resonance energy transfer (FRET) between the donor and acceptor fluorophores conjugated to the antibodies. The signal is in proportion to the target protein level under tested experimental conditions. *Right:* the excitation light of TR-FRET experiments is given as 1- μ s pulses, and thus the background fluorescence from the media or the acceptor decay rapidly, whereas the fluorescence from the donor last for hundreds of μ s, due to the unique property of the donor fluorophore made from lanthanides. When FRET occurs, the acceptor fluorescence lasts longer as well, due to the sustained energy transfer from the donor. A time window could then be selected to measure the FRET dependent signals, which are further calculated by the ratio between the intensity at 665 nm and the one at 615 nm to eliminate the influence from antibody-loading variations, etc. (b) A schematic picture of the epitopes targeted by the different antibodies used in this study.

models^{12,13}. As a result, measuring HTT-exon1 protein levels by TR-FRET is of potential interest in screening in such models.

When measuring HTT-exon1 levels by TR-FRET at the room temperature, the signals from Q72 are much higher than Q25 as expected. Surprisingly, the Q25 signals become very close or even higher than Q72 signals when the assays are performed around 4°C, contradictory to the expected higher apparent affinity of MW1 to the longer polyQ stretch. In other words, the Q25 signals increase much more than Q72 when the temperature is lowered to 4°C. We further investigated this and determined that it is likely due to a temperature-dependent and polyQ length-dependent conformational change of HTT proteins.

Results

HTT TR-FRET signals are influenced by the temperature in a reversible manner. To measure the HTT-exon1 protein levels, we transiently transfected HTT-exon1 Q25 or Q72 expression vector into the HEK293T cells and detected protein expression by Western-blot (5 μ g/lane). The abundance of Q25 protein looks similar to Q72 in the protein lysates from the transfected cells (Fig. 2a) detected by the antibody 2B7, which targets the N-terminus of HTT-exon1 proteins³. As expected, the MW1 detected signals are much weaker for lysates from Q25 transfected cells (Fig. 2b), because MW1 is a polyQ antibody⁶, which has lower apparent affinity to the shorter polyQ stretch in Q25. In addition, heating the samples at 37°C for 1 hour does not seem to change the Western-blot signals (Fig. 2a–b); suggesting no raw abundance change of these proteins. The Western-blot was performed under denaturing conditions, and thus the band intensities may not reflect all the possible structural changes that may have occurred in the cells.

We then measured the HTT-exon1 Q25 and Q72 protein levels in the same lysates or their biological replicates by TR-FRET. By utilizing the 2B7/MW1 and 4C9/MW1 antibody pairs^{3,14,15}, we are able to detect the HTT-exon1 Q25 and Q72 signals (Fig. 2c–e). These

antibody pairs essentially detect only HTT monomers as previously suggested¹⁵. Given that the HEK293T expresses endogenous full length wild-type proteins, we utilized the lysates from non-transfected cells as a background control (Fig. 2c–e). After adding the antibodies, we incubated the plate at room temperature (RT, ~22°C) for 2 hours and then measured the TR-FRET signals (Fig. 2c, RT-1). We then put the plate back to the fridge and incubated it at 4°C for another hour and measured the TR-FRET signals immediately after getting the plate out from the fridge (Fig. 2c, 4C-1) when the plate was still cold. The TR-FRET signals increased under this condition for both Q72 and Q25 proteins (Fig. 2c). We then repeated the temperature shift a few times and observed the same changes in subsequent cycles (Fig. 2c, RT-2, 4C-2 and RT-3). The phenomenon is not present in the non-transfected lysates, because the endogenous full length HTT protein is below the detection limit at the lysate concentrations (Fig. 2c–e) that we tested. Consistent with this, the TR-FRET ratio of non-transfected samples are similar as the no protein lysis buffer controls (~0.15).

The temperature sensitivity of HTT-exon1 Q25 signals is much higher than Q72 signals. The increase of TR-FRET signals at 4°C suggests a negative correlation between the TR-FRET signals and the temperature. Consistent with this, the signals at 37°C is reduced compared to the RT and 4°C (Fig. 2d–e&3a), while the major change occurs between 4°C and RT.

Interestingly, there is an obvious difference in temperature sensitivity of the signals from HTT-exon1 Q25 versus Q72. The fold increase of Q25 signals at 4°C compared to room temperature is much larger than the increase of Q72 signals by the 2B7/MW1 (fold increase: 4.05 ± 0.15 versus 0.86 ± 0.11 , $P < 0.0001$, $t = 17.2$) or 4C9/MW1 (fold increase: 7.19 ± 0.26 versus 1.48 ± 0.15 , $P < 0.0001$, $t = 19.0$) antibody pair (Fig. 3a). This results in a “flip” of the relationship between the Q72 and Q25 signals at 4°C compared to RT, i.e. the Q25 signals at 4°C are higher than Q72 signals (Fig. 2c–d),

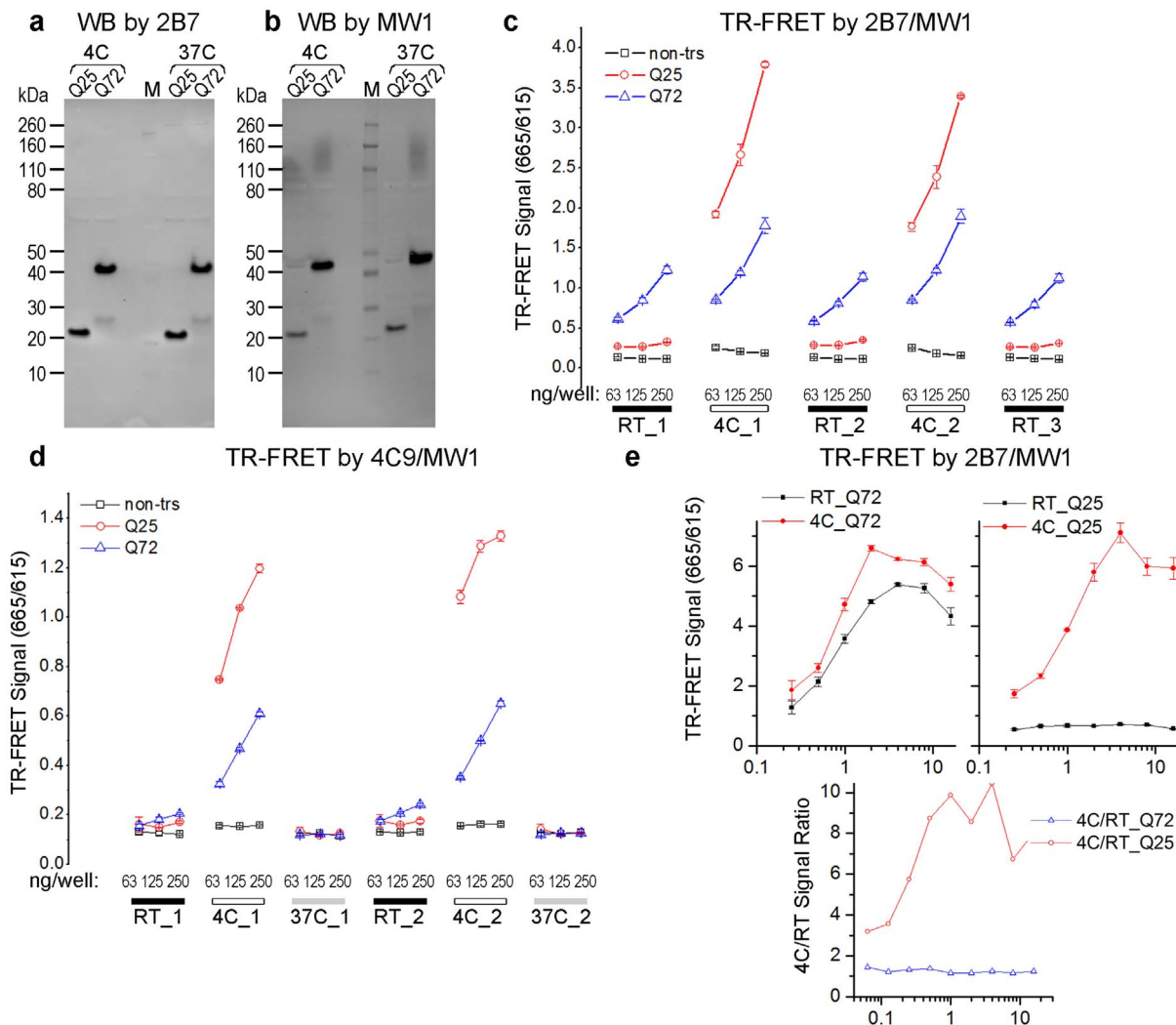


Figure 2 | Different temperature sensitivities of TR-FRET signals of HTT-exon1 proteins. (a) The Western-blot of HTT-exon1 Q72 and Q25, using HTT N-terminal antibody 2B7. (b) The Western-blot using the polyQ antibody MW1 for the same lysates used in (a). (c) 2B7/MW1 TR-FRET signals of the lysates from the transfected cells at 4°C (4C) and room temperature (RT, 22°C). Data plotted as average \pm s.e.m. (n = 3). (d) 4C9/MW1 TR-FRET signals of the lysates from the transfected cells at 4°C (4C), room temperature (RT, 22°C), and 37°C (37C). Data plotted as average \pm s.e.m. (n = 3). (e) *Upper panels*: 2B7/MW1 TR-FRET signals of the Q72 (*left*) and Q25 (*right*) HTT-exon1 transfected samples at different concentrations (μ g/well). Note that the signal plateau has been reached. The *lower panel*: the ratio between 4C and RT for Q72 and Q25 samples at different concentrations (μ g/well). Data plotted as average \pm s.e.m. (n = 4).

contradictory to the fact that the polyQ antibody MW1 has much higher apparent affinity to Q72 than Q25^{6,16} (Fig. 2b). This phenomenon is out of expectation and is caused by a much higher temperature sensitivity of the TR-FRET signals of Q25 than the ones of Q72 between 4°C and RT (Fig. 3a). While the “flip” may not occur at all the different protein concentrations, the temperature sensitivity of the TR-FRET signals of Q25 is larger than the ones of Q72 at all the concentrations tested, including the saturation concentrations (Fig. 2d, Fig. 3c&Fig. 4b). There are several potential explanations for the observed higher temperature sensitivity of the Q25 TR-FRET signals, and are discussed as follows.

Higher temperature sensitivity of HTT-exon1 Q25 is not due to signals coming from proteins other than HTT. One potential explanation is that the increased signal of Q25 at 4°C comes from another protein X. Given that there is no obvious increase of the non-transfected samples and the increase in HTT-exon1 Q72 is much smaller (Fig. 3a), the protein X has to be induced by HTT-exon1 Q25 transfection specifically, sensitive to temperature, and detected by both the 2B7/MW1 and 4C9/MW1 TR-FRET antibody pairs. If

this is true, both 2B7 and 4C9 antibody should bind with protein X in the lysate, and thus the 2B7/4C9 antibody pair should exhibit a similar phenomenon, i.e. the temperature sensitivity of 2B7/4C9 signals should be much higher for Q25 than Q72. Measuring HTT-exon1 proteins by the 2B7/4C9 antibody pair gives HTT-dependent signals (Fig. 3b), suggesting that the assay is able to detect HTT proteins. Meanwhile, the temperature sensitivity of the 2B7/4C9 signals is similar between Q25 and Q72 (Fig. 3a–b; fold increase: 0.10 ± 0.05 versus 0.07 ± 0.04 , $P = 0.63$, $t = 0.48$), and much smaller than the temperature sensitivity of Q25 when using 2B7/MW1 or 4C9/MW1 antibodies. Thus, it is unlikely that the different temperature sensitivity is caused by the involvement of other proteins.

To further exclude the possibility of involvement of other proteins, we tested purified recombinant proteins of the HTT N-terminal fragments, including the HTT-573 fragments (with the first 573 amino acids of HTT⁴) and the N-terminal MBP tagged HTT-exon1 fragments. We observed a higher temperature sensitivity of the signals from Q25 than the ones from Q72 as well (Fig. 3c&Fig. 4b), suggesting that the difference in temperature

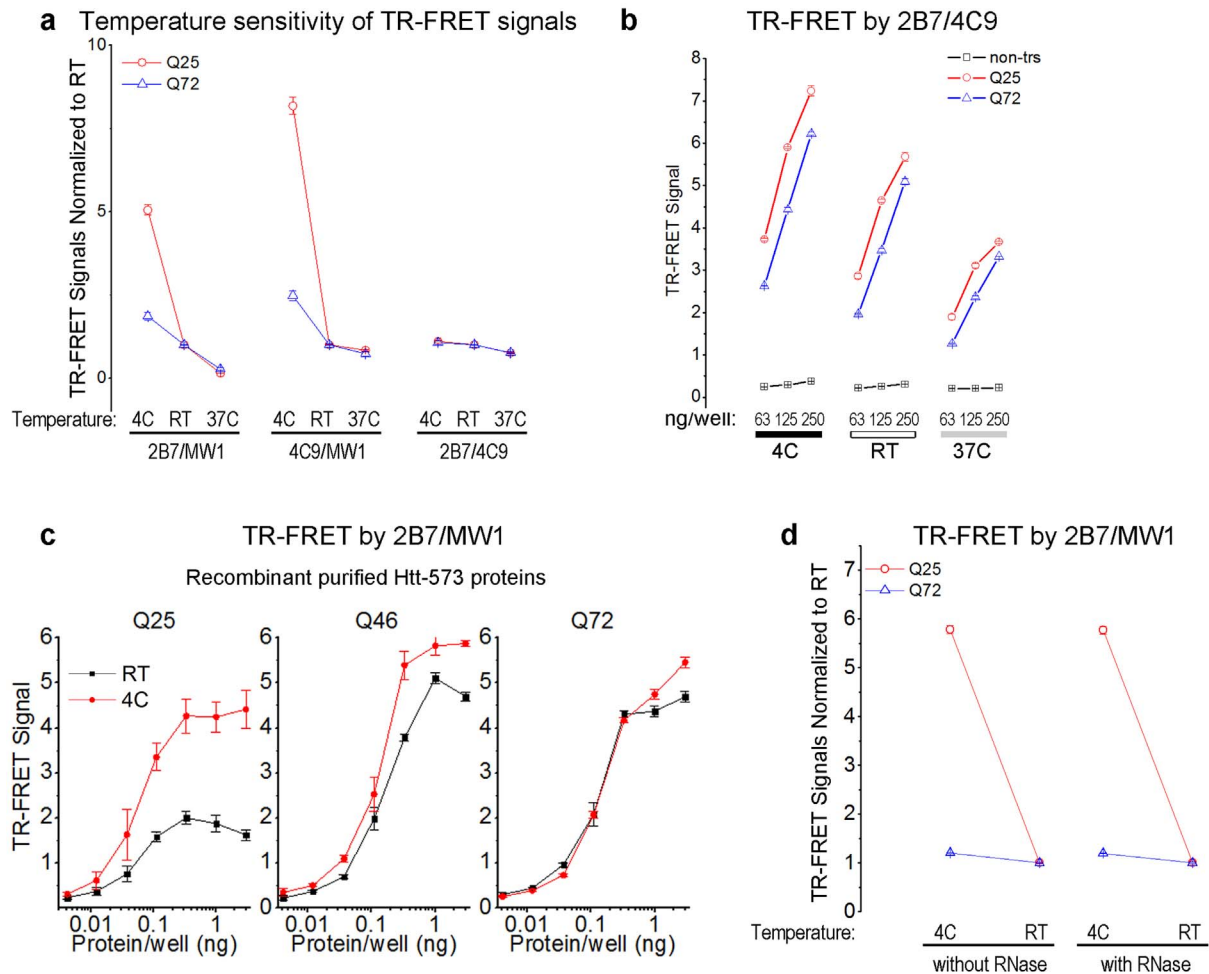


Figure 3 | Higher temperature sensitivity of the Q25 TR-FRET signal is not due to other proteins or HTT protein level changes. (a) Temperature sensitivity of the TR-FRET signals of Q25 versus Q72 HTT-exon1 proteins (125 ng/well) using 2B7/MW1, 4C9/MW1, and 2B7/4C9 TR-FRET antibody pairs. All signals (4°C (4C), room temperature (RT, 22°C), and 37°C (37C)) are normalized to the averaged signal at room temperature (RT) for each protein, $n = 9$, data plotted as average \pm s.e.m. (b) 2B7/4C9 TR-FRET signals of the Q72, Q25 HTT-exon1 transfected samples or the non-transfected samples at 4°C (4C), room temperature (RT), or 37°C (37C). (c) TR-FRET signals of the purified recombinant HTT-573 proteins with different polyQ length (Q25, Q46, Q75) at 4°C (4C) or room temperature (RT). Note that the temperature sensitivity is dependent on the polyQ length: Q25 > Q46 > Q72; $n = 4$, data plotted as average \pm s.e.m. (d) TR-FRET signals of Q25 or Q72 transfected lysates, treated with or without RNase A. $n = 3$, data plotted as average \pm s.e.m.

sensitivity is not due to proteins other than the HTT proteins *per se*.

The Higher temperature sensitivity of HTT-exon1 Q25 is not due to the changes of the raw abundance of the HTT-exon1 proteins.

As discussed above, the signals should come from the transfected HTT-exon1 proteins *per se*. If this is the case, the change of the signals could be explained by the change of the raw abundance of the HTT-exon1 proteins. Given that the changes in TR-FRET signals are almost completely reversible (Fig. 2c–d), both protein degradation and protein synthesis have to be involved, as neither one of them can reverse the effect of itself. In our experiments, we are measuring the TR-FRET signals in the protein lysates with nuclei and organelle fractions discarded, and thus the lysates are not capable of synthesizing new proteins. In addition, we have also added protease inhibitors to block protein degradation. Furthermore, based on Western-blots, we do not observe any decrease of Q25 or Q72 proteins by heating the lysates at 37°C for 1 hour (Fig. 2a–b). Thus, it is highly unlikely that the observed phenomenon is due to the raw abundance changes of the HTT proteins.

To further prove this, we treated the lysates with RNase A to stop all the new protein syntheses, and observed no inhibition on the

temperature sensitivity of Q25 signals (Fig. 3d), confirming that the observed phenomenon is not due to HTT protein level changes. Finally, the recombinant proteins purified from *Escherichia coli* bacterial cultures showed similar phenomenon (Fig. 3c&Fig. 4d), confirming that the observed phenomenon is irrelevant to new protein synthesis or degradation.

Higher temperature sensitivity of HTT-exon1 Q25 is likely due to conformational and solubility changes of the HTT-exon1 proteins.

Besides the HTT-exon1 protein levels, two other major factors that may change TR-FRET signals are the solubility and conformation. It is a tautology that conformation and solubility are likely to inter-connected, and thus it is likely that both of them play a role in the temperature sensitivity of the TR-FRET signals. For example, the saturation concentration of HTT-exon1 fragments increases at lower temperatures, and the degree of increase is polyQ-dependent¹⁷. The changes in solubility may alter antibody binding affinities as well as the HTT conformation, causing the difference in TR-FRET signals. Similarly, Williamson *et al.* proposed that “the degree of intermolecular association increases with increasing polyQ length” based on their simulation data¹⁸. If this is true and the intermolecular association is temperature sensitive between 4°C and the room

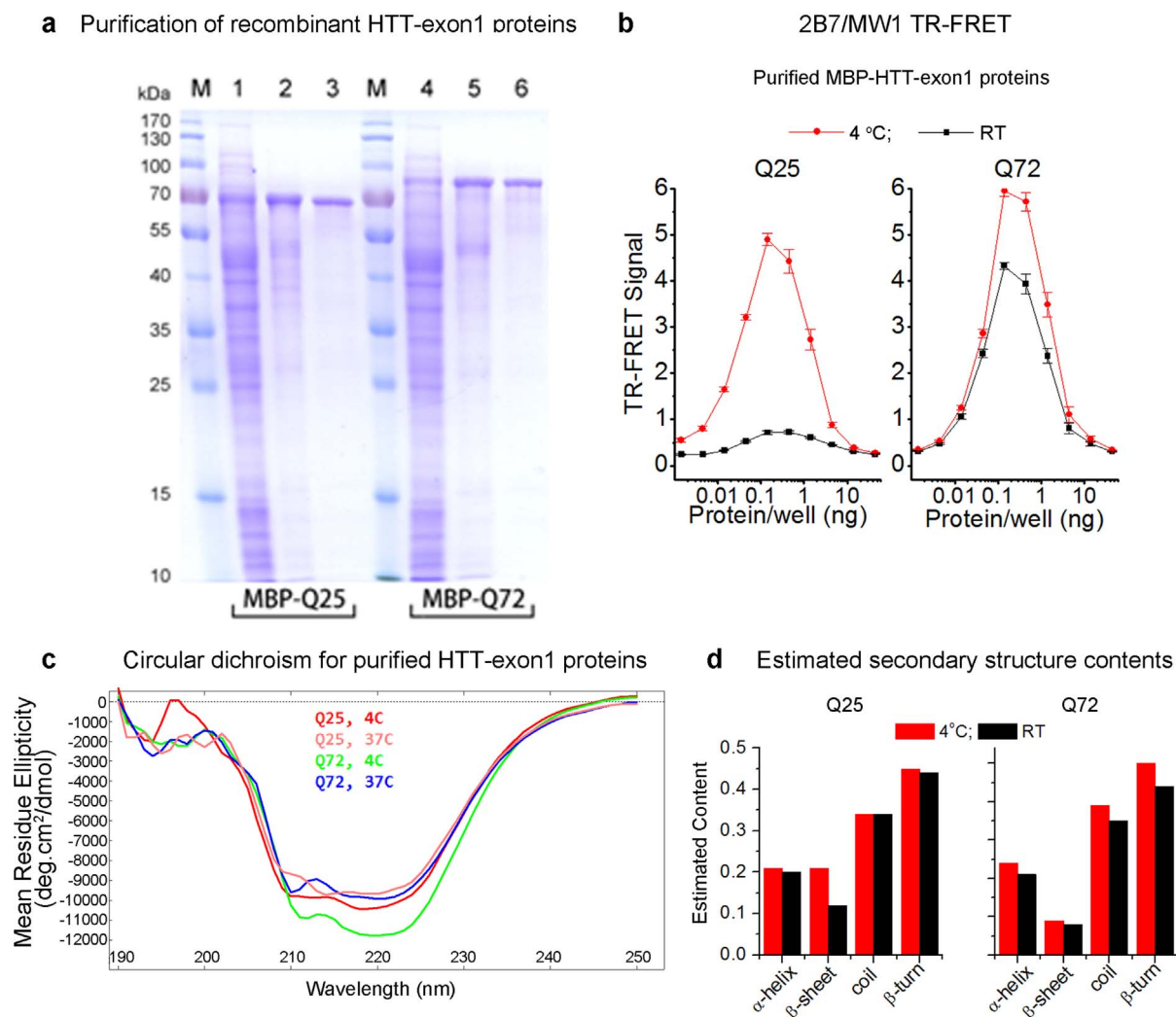


Figure 4 | Conformational analyses of purified recombinant HTT-exon1 proteins. (a) SDS-PAGE analysis of the expression and purification of recombinant MBP tagged HTT-exon1 fusion proteins. Lane 1–3, MBP-Q25, lane 4–6, MBP-Q72. Lane M, the protein molecular weight marker; lane 1 and 4, the supernatants loaded on Ni-NTA column; lane 2 and 5, the eluates of Ni-NTA chromatography; lane 3 and lane 6, the eluates of Superdex 200 size exclusive chromatography for TR-FRET and CD analysis. (b) 2B7/MW1 TR-FRET signals of HTT-exon1 proteins at 4°C and room temperature. Note that the temperature sensitivity is much higher for Q25 than Q72. (c) CD data for the MBP-Q25 and MBP-Q72 at 4°C and 37°C. Red line: MBP-Q25 at 4°C, pink line: MBP-Q25 at 37°C, green line: MBP-Q72 at 4°C, and blue line: MBP-Q72 at 37°C. (d) Estimated secondary structure contents of MBP-Q25 and MBP-Q72 at 4°C and 37°C by the linear regression method.

temperature, it may offer an explanation for temperature and polyQ dependent change of the TR-FRET signals. However, based on this study, the intermolecular association is expected to increase at lower temperatures, and thus likely to decrease the MW1 based TR-FRET signals, contradictory to our observation. In addition, “the degree of intermolecular association increases with increasing polyQ length”¹⁸, and thus TR-FRET signal changes caused by intermolecular association are expected to be larger in Q72 than in Q25, which is also different from our observation. Thus, it is difficult to explain our observations by intermolecular association alone. Williamson *et al.* also presented simulation data showing a temperature- and polyQ length- dependent conformational change between 298 K and 315 K. If similar changes occur at the lower temperature range, it may lead to the TR-FRET signal changes that we have observed.

In order to test if conformational changes play a role in the higher temperature sensitivity of HTT-exon1 Q25 than Q72, we performed circular dichroism (CD) experiments using purified recombinant proteins. We have successfully cloned, expressed and purified MBP tagged HTT-exon1 proteins (Fig. 4a). Same as the tag-free proteins, the temperature sensitivity of 2B7/MW1 TR-FRET signal

is still much higher for MBP-Q25 than MBP-Q72 (Fig. 4b), confirming that these proteins can be used to probe potential causes of the temperature sensitivity. The UV-CD data of MBP-Q25 and MBP-Q72 at 4°C and 37°C were then collected (Fig. 4c). It is noticeable that the shape of the Q25 CD curve exhibits an obvious change (Fig. 4c, red versus pink) when temperature changes, whereas the shape of the Q72 curve remains essentially unchanged (Fig. 4c, blue versus green). The secondary structure contents were further analyzed using the linear regression method developed by Chang *et al.*¹⁹, which was integrated into the DICROPROT program (Fig. 4d). Between 4°C and 37°C, while the α-helix, β-turn and random coil contents have little change, there is a substantial reduction of the β-sheet content of Q25 (from 0.21 to 0.12, decreased 43%). This change is much milder in Q72 (from 0.09 to 0.08; decreased 11%). These results provide a possible explanation of the temperature sensitivity of the TR-FRET signals: the secondary structure (especially the β-sheet) is disturbed when the temperature increases, and this conformational change is much more substantial in Q25, leading to much higher temperature sensitivity of the Q25 TR-FRET signals.

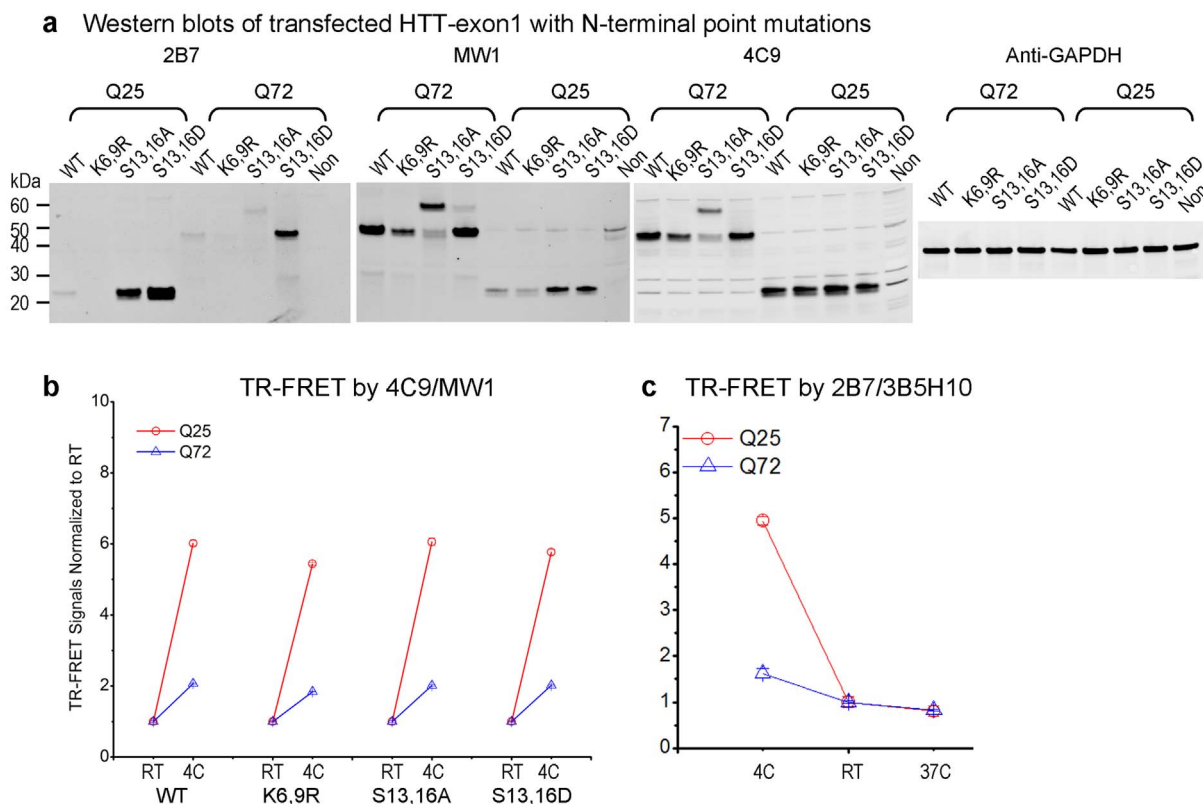


Figure 5 | Higher temperature sensitivity of the Q25 TR-FRET signal is due to structural or spatial changes of HTT polyQ. (a) Western-blots of HEK293T cells transfected with different HTT-exon1 Q25 and Q72 constructs with point mutations as indicated. The last lane on each blot is from non-transfected HEK293T lysate. (b) Temperature sensitivity of the 4C9/MW1 TR-FRET signals. All signals are normalized to the signal at room temperature (RT), $n = 3$. Q25 has higher temperature sensitivity for all the HTT-exon1 constructs with or without point mutations. (c) Temperature sensitivity of the 2B7/3B5H10 TR-FRET signals for Q25 and Q72. All signals are normalized to the signal at room temperature (RT), $n = 6$. Between 4°C and RT, Q25 has higher temperature sensitivity than Q72.

The higher temperature sensitivity is observed by the 2B7/MW1 antibody pair (Fig. 2c), and thus if the observed temperature sensitivity is due to conformational changes, either the 2B7 binding epitope at the N-terminus, or the MW1 binding epitope in the polyQ stretch, or both, undergo(es) temperature-dependent conformational changes. If the conformational change in the N-terminus is the major cause, the phenomenon should be observed by 2B7 paired with other antibodies such as 4C9. The 2B7/4C9 signals however, do not show a higher temperature sensitivity for Q25 than Q72 (Fig. 3a), contradictory to this expectation; suggesting that the phenomenon is unlikely to be due to changes in N-terminus of HTT-exon1 Q25. To further prove this, we have generated a number of point mutations for HTT-exon1 at the N-terminus (Fig. 5a), which are likely to influence the N-terminus structure, as proved by substantial difference in the affinity to the HTT N-terminal antibody 2B7 (Fig. 5a, Western-blots performed for lysates exacted at 4°C). While they have different N-terminal structures, all of them showed the same phenomenon when tested by 4C9/MW1 TR-FRET, and exhibited higher temperature sensitivity in Q25 than Q72 (Fig. 5b); suggesting that the phenomenon is not due to the N-terminus.

The above evidence suggests a possible temperature-dependent change of the antibody affinity or accessibility of the polyQ stretch, and the change needs to be different between Q25 and Q72. We then examined if this is a unique property of the polyQ antibody MW1. We thus tested the same lysates with 2B7-Terbium paired with D2 labeled 3B5H10, another polyQ antibody⁷. Similar phenomenon (Fig. 5c; fold increase: 3.95 ± 0.09 for Q25 versus 0.62 ± 0.10 for Q72, $P < 0.0001$, $t = 24.7$) has been observed with the 2B7/3B5H10 antibody pair; suggesting that the phenomenon is not due to a

temperature dependent change of the antibody MW1, but is more likely due to a structural or spatial change of the polyQ stretch *per se*, which could influence the binding of polyQ antibodies other than MW1.

Taken together, we speculate that the polyQ stretch itself undergoes a polyQ length-dependent structural or spatial change at 4°C, which results in a larger increase of affinity or accessibility of Q25 to the polyQ antibodies such as MW1 and 3B5H10 (Fig. 1). This change is polyQ length dependent and much milder for Q72 proteins (Fig. 2–5). The phenomenon reveals interesting and novel length-dependent and temperature-dependent properties of polyQ that could potentially contribute to understanding its conformation as well as its structural-toxicity relationship. On the other hand, conformation and solubility are likely inter-connected, and it is likely that the degree of supersaturation²⁰ changes at different temperatures¹⁷, and contributes to the temperature sensitivity of the TR-FRET signal as well.

Discussion

In summary, we have discovered that a polyQ length-dependent temperature sensitivity of TR-FRET signals for HTT-exon1 proteins. Based on our analysis above, the sensitivity is likely due to a structural or spatial change of the polyQ stretch at 4°C. Consistent with this, the mutant HTT-exon1 has been reported to have altered conformation and toxicity at 4°C compared to higher temperatures²¹. Interestingly, much higher temperature sensitivity has been observed for HTT-exon1 Q25 than Q72; suggesting substantial difference in the structural or spatial change of short versus long polyQ.

The discovery reminds scientists in the field about the importance of temperatures in TR-FRET experiments and potentially other



immunoassays. It also opens up possibilities of utilizing the technology for detecting conformational changes, as well as distinguishing short polyQ versus long polyQ proteins -- high temperature sensitivity of anti-polyQ antibody based TR-FRET signals may suggest presence of short polyQ proteins, whereas low temperature sensitivity may suggest presence of long polyQ proteins. This might be especially useful for clinical samples when the loadings are very difficult to control. This observation could also be potentially utilized for screenings of modifiers of mutant HTT conformation. More detailed structural biology experiments are needed to reveal the structural or spatial change of polyQ at different temperatures before such purposes could be achieved.

Methods

Plasmid constructs. The human HTT exon1-constructs (Q72 and Q25) were synthesized by Genewiz Inc. and gateway cloned into the pcDNA/Dest40 plasmids (Life Technologies, # 12274-015). The QuickChange® Site-Directed Mutagenesis Kit (Agilent Technologies, #200518) was used to generate the point mutation constructs, and the complete sequences of plasmids have been validated.

Cell culture and transfection. The HEK293T cells were all cultured in DMEM (Life Technologies, #11965) with 10% FBS (Life Technologies, # 10082-147) and maintained at 37°C incubator with 5% CO₂.

Transfection was performed with lipofectamine2000 (Life Technologies, #11668019) using standard forward transfection protocol provided by the manufacturer. The cells were then placed back to the tissue culture incubator and incubated for 48 hours before collection and lysis (see below).

Cell lysis and Western-blot. The cell pellets were collected and lysed on ice for 30 minutes in PBS + 1% Triton X-100 + 1X complete protease inhibitor (Roche, #05892988001), sonicated for 10 seconds, and spun at >20,000 g at 4°C for 10 minutes to remove the nuclei and large cellular organelles. The supernatants were then loaded and transferred onto nitrocellulose membranes for Western-blot.

The HTT antibodies 2B7 and 4C9²³ and the polyQ antibody MW1⁶ have been described previously. Anti-β-Tubulin was purchased from Abcam (#ab6046). Purified recombinant proteins were obtained from Drs. James Palacino and Andreas Weiss at Novartis and were published previously⁴.

Time-resolved fluorescence resonance energy transfer (TR-FRET) assay. The HTRF assays were performed similarly as previously described^{13,17}. Antibodies targeting HTT were custom-labeled by Cisbio Inc. for detection of HTT protein levels. The labeled antibody pairs were then diluted in the TR-FRET buffer: NaH₂PO₄ (50 mM) pH 7.4, NaF (400 mM), BSA (0.1%), Tween-20 (0.05%), 1% Triton X-100 and 1% EDTA-free protease inhibitor (Calbiochem, #539134). The antibody pairs in the HTRF buffer (6 μl) were added to the bulk lysates (9 μl) in each well of the 384 well plates. For all the experiments, protein concentrations (by BCA, Pierce, #23225) were measured to calculate the loading in each well. The donor antibodies (written before “/” in all the antibody pairs mentioned in the text) were all labeled with Terbium cryptate, whereas the acceptor antibodies (written after “/”) were labeled with D2. For all the antibody pairs used for this study, the donor antibody concentration was 0.023 ng/μl and the acceptor antibody concentration was 1.4 ng/μl in the TR-FRET buffer.

The signal ratios between 665 nm and 615 nm have been calculated as the raw TR-FRET signals. The signals could be further linearly transformed by background subtraction and normalization. Given that it is a linear transformation that is the same for both the Q72 and Q25 samples in the same experiments, the transformation will not affect any observations made in this study.

Cloning, expression and purification of the MBP tagged proteins. The recombinant fusion proteins MBP-Q25 and MBP-Q75 were constructed using a modified pMal-c2X vector with poly-His tag. The positive clones were transformed into BL21 (DE3) cells for expression. The cells were grown in 37°C shaker (240 rpm) to OD (600 nm) of 1.0. 1 mM IPTG was then added and the cells were cooled down to 12°C for an additional 20 hrs. The collected cells were lysed by sonication. After centrifugation at 20,000 × g for 20 minutes, the supernatant were first purified by Ni-NTA Superflow column. The Ni-NTA eluates were further concentrated by ultrafiltration and purified by size exclusive column Superdex 200 (buffer system: 10 mM NaH₂PO₄/Na₂HPO₄, pH 7.4). The whole process was analyzed by SDS-PAGE (Fig. 4a) and Western-blot (not shown). The calculated molecular weights of recombinant MBP-Q25 and MBP-Q72 were 58253.4 Da and 64275.5 Da, respectively.

Circular dichroism (CD) analysis. CD spectra were scanned at the far-UV range (190–250 nm) with a CD spectrometer (Model: MOS-450, Bio-Logic Science Instruments) in a 10-mm-pathlength quartz CD cuvette at 4°C and 37°C. The protein concentrations for the CD analysis were 94.5 μg/ml (MBP-Q25) and 104.2 μg/ml (MBP-Q72), respectively. The recombinant proteins were dissolved in 10 mM

NaH₂PO₄/Na₂HPO₄ buffer (pH 7.4). Three scans were averaged to obtain one spectrum. The CD results were expressed in terms of mean molar ellipticity [θ] (degrees·cm²·dmol⁻¹) plotted against the wavelength. The collected data were then analyzed by DICROPROT software²³ and the estimation of the secondary structure was done by the linear regression method developed by Chang *et al.*¹⁹ and integrated into the DICROPROT program.

Statistics. All the numeric data are plotted as average ± s.e.m. Two-tail Student's t test has been used for P value and t value calculations.

- Mathis, G. Rare earth cryptates and homogeneous fluoroimmunoassays with human sera. *Clin Chem* **39**, 1953–1959 (1993).
- Paganetti, P. *et al.* Development of a method for the high-throughput quantification of cellular proteins. *ChemBiochem* **10**, 1678–1688; doi:10.1002/cbic.200900131 (2009).
- Lu, B. *et al.* Identification of NUB1 as a suppressor of mutant Huntington toxicity via enhanced protein clearance. *Nat Neurosci* **16**, 562–570; doi:10.1038/nn.3367 (2013).
- Weiss, A. *et al.* Single-step detection of mutant huntingtin in animal and human tissues: a bioassay for Huntington's disease. *Anal Biochem* **395**, 8–15; doi:10.1016/j.ab.2009.08.001 (2009).
- TheHuntington'sDiseaseCollaborativeResearchGroup. A novel gene containing a trinucleotide repeat that is expanded and unstable on Huntington's disease chromosomes. *Cell* **72**, 971–983; doi:10.1016/0092-8674(93)90585-E (1993).
- Ko, J., Ou, S. & Patterson, P. H. New anti-huntingtin monoclonal antibodies: implications for huntingtin conformation and its binding proteins. *Brain Res Bull* **56**, 319–329; doi:10.1016/S0304-3840(01)00599-8 (2001).
- Miller, J. *et al.* Identifying polyglutamine protein species in situ that best predict neurodegeneration. *Nat Chem Biol* **7**, 925–934; doi:10.1038/nchembio.694 (2011).
- Li, P. *et al.* The structure of a polyQ-anti-polyQ complex reveals binding according to a linear lattice model. *Nat Struct Mol Biol* **14**, 381–387; doi:10.1038/nmsb1234 (2007).
- Bennett, M. J. *et al.* A linear lattice model for polyglutamine in CAG-expansion diseases. *Proc Natl Acad Sci U S A* **99**, 11634–11639; doi:10.1073/pnas.182393899 (2002).
- Landles, C. *et al.* Proteolysis of mutant huntingtin produces an exon 1 fragment that accumulates as an aggregated protein in neuronal nuclei in Huntington disease. *J Biol Chem* **285**, 8808–8823; doi:10.1074/jbc.M109.075028 (2010).
- Sathasivam, K. *et al.* Aberrant splicing of HTT generates the pathogenic exon 1 protein in Huntington disease. *Proc Natl Acad Sci U S A* **110**, 2366–2370; doi:10.1073/pnas.1221891110 (2013).
- Mangiarini, L. *et al.* Exon 1 of the HD gene with an expanded CAG repeat is sufficient to cause a progressive neurological phenotype in transgenic mice. *Cell* **87**, 493–506; doi:10.1016/0092-8674(00)81369-0 (1996).
- Lu, B. & Palacino, J. A novel human embryonic stem cell-derived Huntington's disease neuronal model exhibits mutant huntingtin (mHTT) aggregates and soluble mHTT-dependent neurodegeneration. *FASEB J* **27**, 1820–1829; doi:10.1096/fj.12-219220 (2013).
- Baldo, B. *et al.* A screen for enhancers of clearance identifies huntingtin as a heat shock protein 90 (Hsp90) client protein. *J Biol Chem* **287**, 1406–1414; doi:10.1074/jbc.M111.294801 (2012).
- Baldo, B. *et al.* TR-FRET-Based Duplex Immunoassay Reveals an Inverse Correlation of Soluble and Aggregated Mutant huntingtin in Huntington's Disease. *Chemistry & Biology* **19**, 264–275; doi:10.1016/j.chembiol.2011.12.020 (2012).
- Legleiter, J. *et al.* Monoclonal antibodies recognize distinct conformational epitopes formed by polyglutamine in a mutant huntingtin fragment. *J Biol Chem* **284**, 21647–21658; doi:10.1074/jbc.M109.016923 (2009).
- Cricka, S. R. K., Garaia, K., Friedenb, C. & Pappua, R. Unmasking the roles of N- and C-terminal flanking sequences from exon 1 of huntingtin as modulators of polyglutamine aggregation. *Proc Natl Acad Sci U S A* **110**, 20075–20080; doi:10.1073/pnas.1320626110 (2013).
- Williamson, T. E., Vitalis, A., Crick, S. L. & Pappua, R. V. Modulation of polyglutamine conformations and dimer formation by the N-terminus of huntingtin. *J Mol Biol* **396**, 1295–1309; doi:10.1016/j.jmb.2009.12.017 (2010).
- Chang, C. T., Wu, C. S. & Yang, J. T. Circular dichroic analysis of protein conformation: inclusion of the beta-turns. *Anal Biochem* **91**, 13–31; doi:0003-2697(78)90812-6 (1978).
- Ciryam, P., Tartaglia, G. G., Morimoto, R. I., Dobson, C. M. & Vendruscolo, M. Widespread aggregation and neurodegenerative diseases are associated with supersaturated proteins. *Cell Rep* **5**, 781–790; doi:10.1016/j.celrep.2013.09.043 (2013).
- Nekooki-Machida, Y. *et al.* Distinct conformations of in vitro and in vivo amyloids of huntingtin-exon1 show different cytotoxicity. *Proc Natl Acad Sci U S A* **106**, 9679–9684; doi: 10.1073/pnas.0812083106 (2009).
- Weiss, A., Rosci, A. & Paganetti, P. Inducible mutant huntingtin expression in HN10 cells reproduces Huntington's disease-like neuronal dysfunction. *Mol Neurodegener* **4**, 11; doi: 10.1186/1750-1326-4-11 (2009).



23. Deleage, G. & Geourjon, C. An interactive graphic program for calculating the secondary structure content of proteins from circular dichroism spectrum. *Comput Appl Biosci* **9**, 197–199; 10.1093/bioinformatics/9.2.197 (1993).

Acknowledgments

We'd like to thank Drs. James Palacino and Andreas Weiss at Novartis for providing us the plasmids, the purified recombinant HTT-573 proteins and the TR-FRET antibodies for this study. We'd also like to thank Dr. James Palacino for critical reading of the manuscript. Finally, we'd like to thank Chinese Ministry of Science and Technology (2014AA02502), Nature Science Foundation of China (NSFC 31371421) and Shanghai Pujiang Talent Plan (13PJ1400600) for funding supports.

Author contributions

B.L. made the original observation; L.Y., L.M., C.X. and B.L. performed the TR-FRET and Western-blot experiments; Q.L. and Y.D. performed the structural experiments; B.L. and Y.D. wrote the manuscript.

Additional information

Competing financial interests: The authors declare no competing financial interests.

How to cite this article: Cui, X. *et al.* TR-FRET Assays of Huntingtin Protein Fragments Reveal Temperature and PolyQ Length-Dependent Conformational Changes. *Sci. Rep.* **4**, 5601; DOI:10.1038/srep05601 (2014).



This work is licensed under a Creative Commons Attribution-NonCommercial-ShareAlike 4.0 International License. The images or other third party material in this article are included in the article's Creative Commons license, unless indicated otherwise in the credit line; if the material is not included under the Creative Commons license, users will need to obtain permission from the license holder in order to reproduce the material. To view a copy of this license, visit <http://creativecommons.org/licenses/by-nc-sa/4.0/>